Calcium and cAMP levels interact to determine attraction versus repulsion in axon guidance

Elizabeth M Forbes[1], Andrew W Thompson[1], Jiajia Yuan[1] and Geoffrey J Goodhill[1,2]
[1]Queensland Brain Institute & [2]School of Mathematics and Physics, The University of Queensland, St Lucia, QLD 4072, Australia

Supplemental Materials

Supplemental Table/Figures

Supplemental Table 1: Parameter values used in the model (related to Fig. 1). These are taken primarily from Graupner and Brunel (2007).

Supplemental Figure 1: The relationship between calcium and all other components of the model (related to Fig. 1). Note the bimodal nature of CaMKII activation in panel **B**. As calcium levels increase the CaMKII:CaN ratio first decreases due to the gradual rise in CaN levels, but then suddenly increases as CaMKII levels suddenly increase. CaMKII levels then rapidly saturate, and the ratio continues to decline as CaN continues its steady increase. Note that PKA activity (panel **D**) and I1 concentrations (panel **E**) are plotted on log scales, in order to make small changes more visible.

Supplemental Figure 2: Illustration of adjustment of resting calcium level, and the effect of including PP1 as a mediator of repulsion (related to Figs. 2,3). A. The CaMKII:CaN ratio plotted against calcium concentration as in Fig. 2A, but with parametter CaM_0 reduced so that resting calcium is now approximately 0.4μM. **B.** The ratio of CaMKII:CaN ratios between two compartments plotted against calcium as in Fig. 3A but with CaM_0 reduced as in panel A. This illustrates that the basic predictions of the model regarding the effect of raising or lowering calcium and cAMP levels relative to their normal resting levels are robust to variations in the particular normal resting calcium level. **C,D.** The ratio of CaMKII:CaN-PP1 ratios between two compartments plotted against calcium with a 30% difference in calcium between the two compartments. **C.** Including PP1 in the ratio has no effect on the turning outcome at resting and low calcium levels (points L and H cf Fig. 2C points L and H). However at high calcium levels the model now predicts attraction. **D.** Normalizing the CaN and PP1 levels included in the ratio leads to the same prediction at each calcium level as when PP1 is not included.

Supplemental Figure 3: The effect of diffusion on the model (related to Figs. 2,3). The ratio of CaMKII:CaN ratios between two compartments for an attractive cue plotted against calcium concentration (cf Fig. 2C) for different levels of diffusion for various molecules between the two compartments. **A.** CaM. **B.** I1. **C.** PP1. **D.** PKA. It can be seen that small amounts of diffusion (e.g. $P = 0.1$, see Methods) do not affect the fundamental behavior of the model for CaM, I1 and PP1. A stronger effect of diffusion is seen for PKA, but in reality the diffusion of PKA/cAMP is probably very limited (see main text).

Parameter	Value	Parameter	Value
K_1	$0.1\mu M$	k^0_{CaN}	$0.1s^{-1}$
K_2	$0.025\mu M$	k_{CaN}	$18s^{-1}$
K_3	$0.32\mu M$	n_{CaN}	3
K_4	$0.4\mu M$	K_{CaN}	$0.053\mu M$
K_5	$0.1\mu M$	k^0_{PKA}	$0.00359s^{-1}$
k_6	$6s^{-1}$	k_{PKA}	$10 - 1000s^{-1}$
k_7	$6s^{-1}$	n_{PKA}	8
k_8	$6s^{-1}$	K_{PKA}	$0.11\mu M$
k_{11}	$100s^{-1}$	K_M	$0.45\mu M$
k_{12}	$6000s^{-1}$	$D + D_I$	$0.2\mu M$
k_{13}	$500s^{-1}$	I_0	$1\mu M$
k_{14}	$0.1s^{-1}$	CaM_0	$2.5\mu M$
		$CaMKII$	$16.67\mu M$

Table 1:

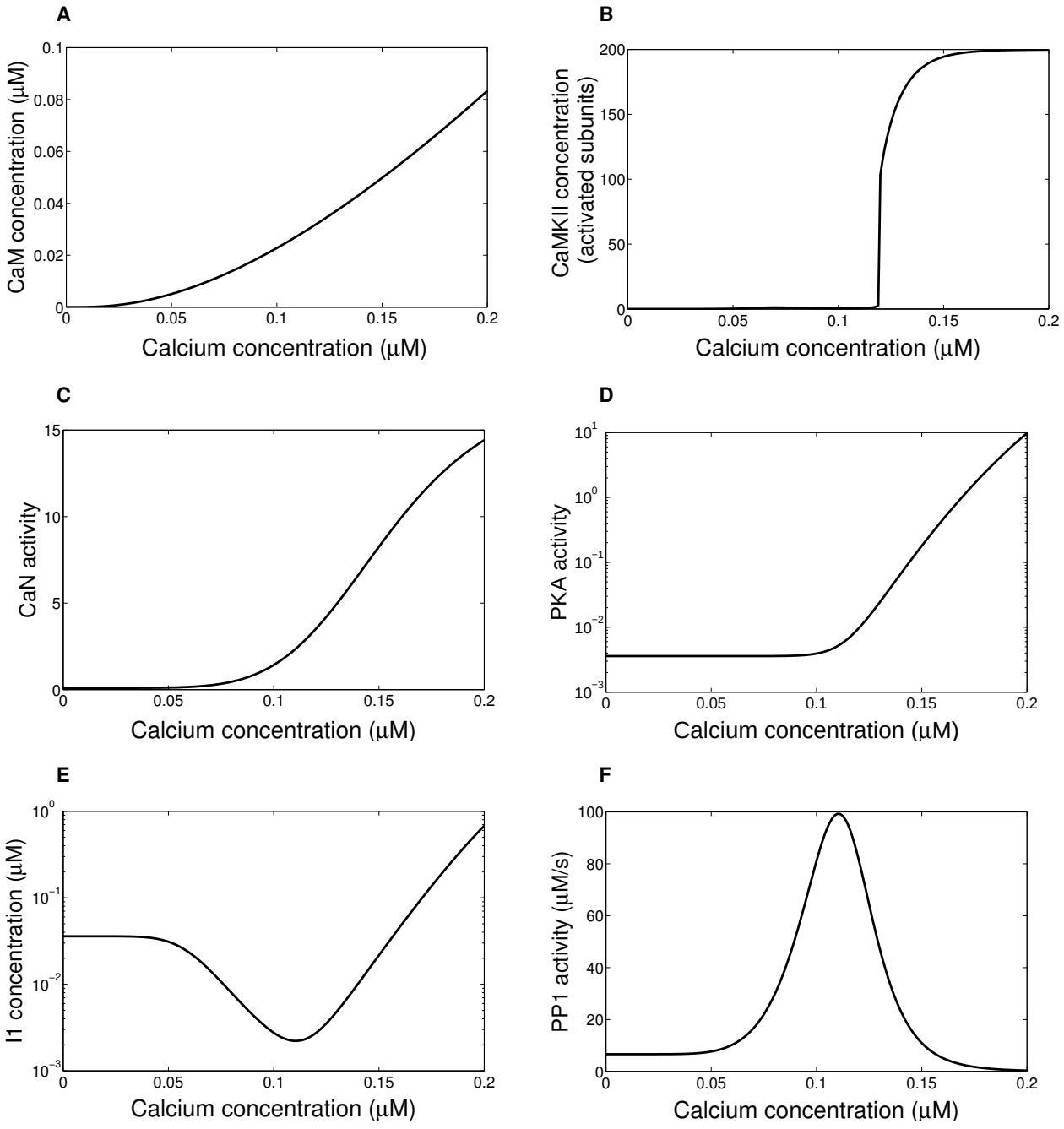
A
CaM concentration (μM)
Calcium concentration (μM)
B
CaMKII concentration (activated subunits)
Calcium concentration (μM)
C
CaN activity
Calcium concentration (μM)
D
PKA activity
Calcium concentration (μM)
E
I1 concentration (μM)
Calcium concentration (μM)
F
PP1 activity (μM/s)
Calcium concentration (μM)

Figure 1:

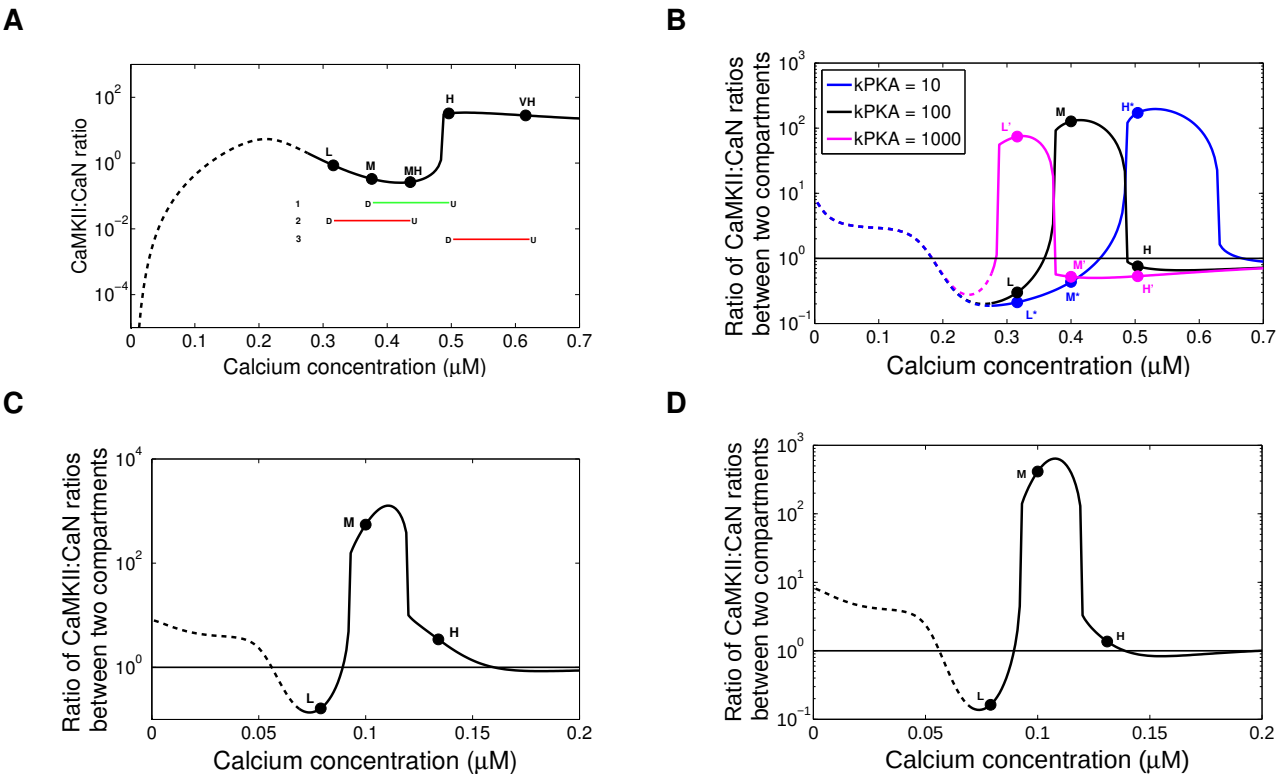
A
B
C
D
CaMKII:CaN ratio
Calcium concentration (μM)
L
M
MH
H
VH
1
2
3
D
U
Ratio of CaMKII:CaN ratios between two compartments
kPKA = 10
kPKA = 100
kPKA = 1000
L'
M'
H'
L*
M*
H*

Figure 2:

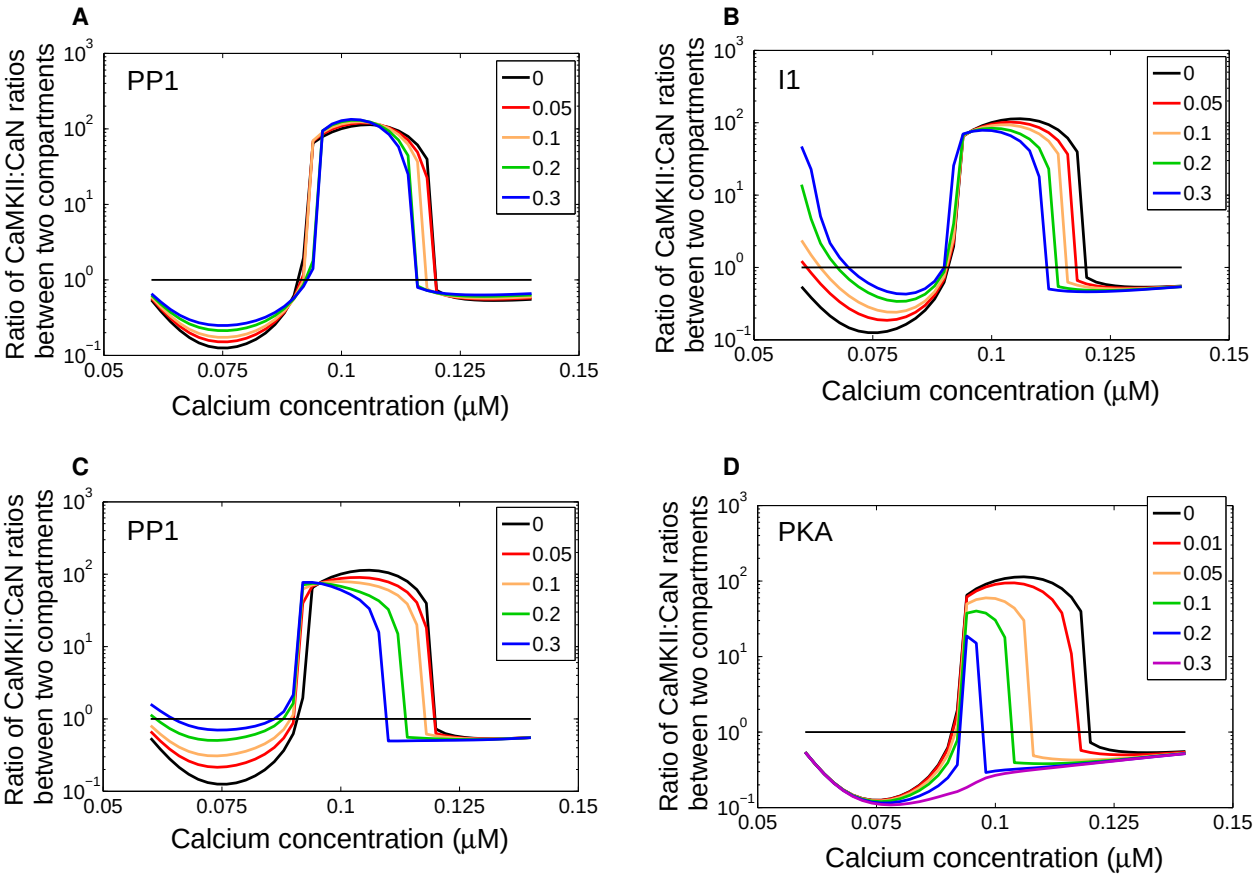
A
PP1
0
0.05
0.1
0.2
0.3
Ratio of CaMKII:CaN ratios between two compartments
Calcium concentration (μM)
B
I1
C
PP1
D
PKA
0.01

Figure 3:

Supplemental Methods

Mathematical methods

The model used is adapted from the model proposed by Graupner and Brunel (2007) for the switch between LTP and LTD. Other similar models have also been used to model the role of CaMKII activation during LTP/LTD (reviewed in Manninen et al. (2010)). We extended the model to two compartments in order to provide a 'distribution' of inputs and outputs over the growth cone. This allows the determination of whether each combination of calcium, cAMP, and spatially non-uniform calcium influx results in attraction or repulsion.

Notation. We use similar notation and parameter values to those of Graupner and Brunel (2007) (given in Supplemental Table 1). Note that while the symbol k is used to signify a rate constant and K is used to signify a dissociation constant, they share the same system of numbering (e.g. $\ldots K_5, k_6, k_7, k_8, K_9, k_{10} \ldots$ etc).

Calcium calmodulin binding. Calmodulin (CaM) has four binding sites for calcium (Linse et al., 1991). Binding to these sites occurs in a co-operative manner as described in the following scheme:

$$C_0 \overset{Ca^{2+}}{\underset{K_1}{\rightleftharpoons}} C_1 \overset{Ca^{2+}}{\underset{K_2}{\rightleftharpoons}} C_2 \overset{Ca^{2+}}{\underset{K_3}{\rightleftharpoons}} C_3 \overset{Ca^{2+}}{\underset{K_4}{\rightleftharpoons}} C \tag{1}$$

Here C_x indicates calmodulin bound with x calcium ions and C is calmodulin bound with four ions. Note that only the macroscopic binding is considered, not the individual binding sites of calcium. For the purpose of this model only calmodulin bound with four calcium ions (C) will be considered to be active in the autophosphorylation of CaMKII, as partially bound calmodulin produces negligible effects (Zhabotinsky, 2000). As binding of calcium by calmodulin is faster than that of other calcium binding proteins (Faas et al., 2011), all the bound states of calmodulin are considered to be in equilibrium with the calcium concentration. Initially it is assumed that all the calmodulin is free, i.e. $C_1 = C_2 = C_3 = C = 0$. This leads to the system of coupled ordinary differential equations:

$$\dot{C}_0 = K_1 C_1 - 4Ca.C_0 \tag{2}$$
$$\dot{C}_1 = 4Ca.C_0 - K_1 C_1 + 2K_2 C_2 - 3Ca.C_1 \tag{3}$$
$$\dot{C}_2 = 3Ca.C_1 - 2K_2 C_2 + 3K_3 C_3 - 2Ca.C_2 \tag{4}$$
$$\dot{C}_3 = 2Ca.C_2 - 3K_3 C_3 + 4K_4 C - Ca.C_3 \tag{5}$$
$$\dot{C} = Ca.C_3 - 4K_4 C \tag{6}$$

where Ca is the concentration of calcium. Due to the fast buffering activity of calmodulin (Faas et al., 2011) this system is solved before any of the other equations, so that C is constant in the following equations.

Autophosphorylation of CaMKII. The CaMKII holoenzyme has 6 functional subunits in a ring (Bradshaw et al., 2002) (Fig. 1B). Calcium/calmodulin binding to adjacent subunits in the ring stimulates

intersubunit phosphorylation (Hudmon and Schulman, 2002). One subunit acts as a subtrate and the next subunit acts as a catalyst. A calcium/calmodulin complex has to be bound to the substrate subunit for autophosphorylation to occur. The catalytic subunit can be in one of three states: bound with calcium/calmodulin, phosphorylated, or phosphorylated and bound with calcium/calmodulin (Lisman et al., 2002).

Let γ be the probability that C (calmodulin bound with 4 calcium ions) binds to a dephosphorylated CaMKII subunit, and γ^* be the probability that C binds to a phosphorylated subunit. Let S and S^* denote dephosphorylated and phosphorylated CaMKII subunits respectively, and SC and S^*C be calcium/calmodulin bound subunits. Assuming that the binding of C is at equilibrium, and taking K_5 and K_9 as the dissociation constants of the respective reactions, then applying the Law of Mass Action yields the following equations for γ and γ^*.

$$\gamma = \frac{SC}{S + SC} = \frac{C}{K_5 + C} \tag{7}$$

$$\gamma^* = \frac{S^*C}{S^* + S^*C} = \frac{C}{K_9 + C} \tag{8}$$

Assuming no calmodulin consumption, then the probability that the substrate subunit is phosphorylated in a unit time in a single direction depends on the state of the catalytic subunit. If the catalytic unit is bound to C then the probability is $k_6\gamma^2$. If the catalytic unit is phosphorylated then the probability is $k_8\gamma(1-\gamma^*)$. If the catalytic unit is bound and phosphorylated then the probability is $k_7\gamma\gamma^*$.

Dephosphorylation of CaMKII. The dephosphorylation of CaMKII is mediated by the protein phosphatase PP1. Let D denote the concentration of active PP1, then the dephosphorylation is described as follows:

$$S^* + D \underset{k_{-11}}{\overset{k_{11}}{\rightleftharpoons}} S^*.D \overset{k_{12}}{\rightarrow} S + D \tag{9}$$

$$S^*C + D \underset{k_{-11}}{\overset{k_{11}}{\rightleftharpoons}} S^*C.D \overset{k_{12}}{\rightarrow} SC + D \tag{10}$$

Note that dephosphorylation occurs regardless of whether a subunit is bound or not to C. Using the standard Michaelis-Menten equation the per-subunit rate of dephosphorylation, k_{10}, is

$$k_{10} = \frac{k_{12}D}{K_M + S_{active}} \tag{11}$$

Here the dissociation constant is given by $K_M = \frac{k_{-11}+k_{12}}{k_{11}}$ and S_{active} is the total concentration of phophorylated subunits.

Applying the Law of Mass action, taking into account the geometry of the CaMKII six-subunit ring and noting that as $k_7 = k_8$ we can simplify $k_7\gamma\gamma^* + k_8\gamma(1-\gamma^*) = k_7\gamma$, the autophosphorylation and dephosphorylation by PP1 is then given by the following system of coupled ordinary differential equations.

$$
\begin{aligned}
\dot{S}_0 &= \dot{S}_{000000} &&= -6k_6\gamma^2 S_0 + k_{10}S_1 \\
\dot{S}_1 &= \dot{S}_{100000} &&= 6k_6\gamma^2 S_0 - 4k_6\gamma^2 S_1 - k_7\gamma S_1 - k_{10}S_1 + 2k_{10}(S_2 + S_3 + S_4) \\
\dot{S}_2 &= \dot{S}_{110000} &&= k_6\gamma^2 S_1 + k_7\gamma S_1 - 3k_6\gamma^2 S_2 - k_7\gamma S_2 - 2k_{10}S_2 + k_{10}(2S_5 + S_6 + S_7) \\
\dot{S}_3 &= \dot{S}_{101000} &&= 2k_6\gamma^2 S_1 - 2k_6\gamma^2 S_3 - 2k_7\gamma S_3 - 2k_{10}S_3 + k_{10}(S_5 + S_6 + S_7 + 3S_8) \\
\dot{S}_4 &= \dot{S}_{100100} &&= k_6\gamma^2 S_1 - 2k_6\gamma^2 S_4 - 2k_7\gamma S_4 - 2k_{10}S_4 + k_{10}(S_6 + S_7) \\
\dot{S}_5 &= \dot{S}_{111000} &&= k_6\gamma^2 S_2 + k_7\gamma(S_2 + S_3) - 2k_6\gamma^2 S_5 - k_7\gamma S_5 - 3k_{10}S_5 + k_{10}(2S_9 + S_{10}) \\
\dot{S}_6 &= \dot{S}_{110100} &&= k_6\gamma^2(S_2 + S_3) + 2k_7\gamma S_4 - k_6\gamma^2 S_6 - 2k_7\gamma S_6 - 3k_{10}S_6 \\
& & &\quad + k_{10}(S_9 + S_{10} + 2S_{11}) \\
\dot{S}_7 &= \dot{S}_{110010} &&= k_6\gamma^2(S_2 + 2S_4) + k_7\gamma S_3 - k_6\gamma^2 S_7 - 2k_7\gamma S_7 - 3k_{10}S_7 + k_{10}(S_9 + S_{10} + 2S_{11}) \\
\dot{S}_8 &= \dot{S}_{101010} &&= k_6\gamma^2 S_3 - 3k_7\gamma S_8 - 3k_{10}S_8 + k_{10}S_{10} \\
\dot{S}_9 &= \dot{S}_{111100} &&= k_6\gamma^2 S_5 + k_7\gamma(S_5 + S_6 + S_7) - k_6\gamma^2 S_9 - k_7\gamma S_9 - 4k_{10}S_9 + 2k_{10}S_{12} \\
\dot{S}_{10} &= \dot{S}_{111010} &&= k_6\gamma^2(S_5 + S_6) + k_7\gamma(S_7 + 3S_8) - 2k_7\gamma S_{10} - 4k_{10}S_{10} + 2k_{10}S_{12} \\
\dot{S}_{11} &= \dot{S}_{110110} &&= k_6\gamma^2 S_7 + k_7\gamma S_6 - 2k_7\gamma S_{11} - 4k_{10}S_{11} + k_{10}S_{12} \\
\dot{S}_{12} &= \dot{S}_{111110} &&= k_6\gamma^2 S_9 + k_7\gamma(S_9 + 2S_{10} + 2S_{11}) - k_7\gamma S_{12} - 5k_{10}S_{12} + 6k_{10}S_{13} \\
\dot{S}_{13} &= \dot{S}_{111111} &&= k_7\gamma S_{12} - 6k_{10}S_{13}
\end{aligned}
$$

where S_i is one of the macroscopic activation states of CaMKII and the subscript in the second term shows the geometrical order of the phosphorylated site in the CaMKII ring.

Calcium-dependent PP1 activity. The activity of PP1 is directly inhibited by phosphorylated inhibitor 1 (I1), which in turn is phosphorylated by cAMP-dependent PKA and dephosphorylated by the phosphatase CaN (Henley and Poo, 2004). This can be written as

$$I_G \underset{v_{CaN}(C)}{\overset{v_{PKA}(C)}{\rightleftharpoons}} I \tag{12}$$

$$I + D \underset{k_{14}}{\overset{k_{13}}{\rightleftharpoons}} D_I \tag{13}$$

where I_G is dephosphorylated I1, I is phosphorylated I1, D is free PP1 and D_I is inhibited PP1.

The phosphorylation (v_{PKA}) and dephosphorylation (v_{CaN}) rate of I1 is calcium/calmodulin-dependent and each can be described by a Hill equation (Stemmer and Klee, 1994):

$$v_{CaN}(C) = k^0_{CaN} + \frac{k_{CaN}}{1 + \left(\frac{K_{CaN}}{C}\right)^{n_{CaN}}} \tag{14}$$

$$v_{PKA}(C) = k^0_{PKA} + \frac{k_{PKA}}{1 + \left(\frac{K_{PKA}}{C}\right)^{n_{PKA}}} \tag{15}$$

where k^0_x is calcium/calmodulin-independent base activity, k_x is the maximal calcium/calmodulin-

dependent activity, K_x is the half-activity concentration, and n_x is the Hill coefficient.

Taking into account PP1 conservation and applying the Law of Mass action yields

$$\dot{I} = -k_{13}I.D + k_{14}D_I - v_{CaN}(C)I + v_{PKA}(C)I_0 \quad (16)$$

$$\dot{D} = -k_{13}I.D + k_{14}D_I \quad (17)$$

Here I_0 refers to the total I1 concentration and is not conserved. Initially it is assumed that all the PP1 is free, ie $D_I = 0$, and all the I1 is inactive ie $I_{t=0} = 0$. Plots of the levels of each of the signaling components versus calcium concentration are shown in Fig. S1.

cAMP vs cGMP. In the model cAMP is not explicitly represented; rather we use the activity of PKA to reflect the concentration of cAMP. However another cyclic nucleotide, cGMP, is also involved in axon guidance and it is the ratio of cAMP to cGMP that determines attraction or repulsion (Song et al., 1998; Song and Poo, 1999; Nishiyama et al., 2003). For simplicity we assume that decreasing cGMP has the same effect as increasing cAMP and vice versa, and do not explicitly include cGMP levels in our model.

Two compartment model. In order to determine whether a change in calcium across the growth cone results in attraction or repulsion it is necessary to include a spatial component in the model. The simplest and most computationally efficient way to include a spatial component is to consider two compartments representing the left and right side of the growth cone. Reactions are assumed to be well-stirred within each compartment, so that each compartment functions as a single point in space. In general each compartment has a different calcium concentration due to a different concentration of ligand, and thus a direct comparison of the ratio of phosphorylated CaMKII subunits to CaN activity can be made between the two compartments. We assume that the growth cone turns towards the compartment with the highest CaMKII:CaN ratio. We also initially assume that the reactions occur fast enough that diffusion between the two compartments does not need to be considered (see Diffusion section below). When determining the calcium inputs for the two compartments, we assume that a steep gradient ($\approx$ 10% change in ligand concentration across the width of the growth cone) is amplified to produce a 30% change in calcium concentration between the two compartments for an attractive guidance cue, and a 10% change in calcium concentration for a repulsive guidance cue. The model requires a large difference in calcium between the two compartments in order to achieve a significant range of calcium values at which attraction will occur.

Diffusion. We also tested the robustness of the model to diffusion between the two compartments. We incorporated diffusion of calmodulin and/or PKA, and thus by extension cAMP, by sharing a proportion P of the difference in concentration between the two compartments (A and B for the up- and down- gradient compartments respectively) at each time step, defined as

$$A_{t+1} = A_t - P(A_t - B_t) \quad (18)$$

$$B_{t+1} = B_t + P(A_t - B_t) \quad (19)$$

Thus $P = 0.5$ corresponds to equalising the concentrations between the two compartments at each step. We considered P in the range of $0 - 0.3$. Since our model is expressed independently of any absolute length or time scales P cannot easily be compared directly with a diffusion rate.

Resting calcium level. We assumed that the normal resting calcium level in the model is approximately 0.1μM, and chose parameter values so that at this point a small increase in calcium results in repulsion, but a large increase results in attraction in the model (see Figs. 2A and 2B). This value is within the range estimated for a variety of neurons by Henley and Poo (2004), but is not critical for the model (see Parameter Sensitivity in Results).

Stochastic binding of ligand The response of a growth cone to a guidance cue is not deterministic: growth cones that otherwise appear similar usually follow different trajectories when confronted with the same guidance cue. To address this we extended the model to consider the probabilistic binding of a ligand. We assumed the probability of a ligand binding to a receptor is $\frac{c}{c+k_{15}}$ where c is the local concentration of the ligand and k_{15} is the dissociation constant. For a compartment with n receptors the binomial distribution can be used to find a probability for the number of receptors bound in each compartment. Thus, given an external concentration gradient for the ligand (e.g. 10%), the true difference between compartments results in a distribution of perceived differences. Indeed it is possible for the compartment with a higher concentration of ligand to actually have a lower number of bound receptors (Berg and Purcell, 1977). We assumed that the calcium concentration in each compartment is linearly related to the number of ligand receptors bound, and ran a Monte Carlo simulation to determine the probability of attraction versus repulsion. In addition to receptor binding noise, there is also downstream signaling noise due to the Brownian motion of the limited number of protein copies available. However even for molecules with very low concentrations in the model (1μM) there are of the order of 10^6 molecules in a 10μm cube, with an expected fractional fluctuation of $\sqrt{10^6}/10^6 = 0.1\%$. Thus the contribution of thermal noise in the downstream signaling is much less than that of receptor binding noise.

Numerical methods. The systems of coupled differential equations were solved using ode15s in MATLAB.

References

Berg, H. C. and Purcell, E. M. (1977). Physics of chemoreception. *Biophysical journal*, 20(2):193–219.

Bradshaw, J. M., Hudmon, A., and Schulman, H. (2002). Chemical quenched flow kinetic studies indicate an intraholoenzyme autophosphorylation mechanism for Ca2+/calmodulin-dependent protein kinase II. *The Journal of Biological Chemistry*, 277(23):20991–20998.

Faas, G. C., Raghavachari, S., Lisman, J. E., and Mody, I. (2011). Calmodulin as a direct detector of Ca2+ signals. *Nature Neuroscience*, 14(3):301–304.

Graupner, M. and Brunel, N. (2007). STDP in a bistable synapse model based on CaMKII and associated signaling pathways. *PLoS computational biology*, 3(11):2299–2323.

Henley, J. and Poo, M.-m. (2004). Guiding neuronal growth cones using Ca2+ signals. *Trends in Cell Biology*, 14(6):320–30.

Hudmon, A. and Schulman, H. (2002). Structure-function of the multifunctional Ca2+/calmodulin-dependent protein kinase II. *The Biochemical Journal*, 364(3):593–611.

Linse, S., Helmersson, A., and Forsén, S. (1991). Calcium binding to calmodulin and its globular domains. *The Journal of Biological Chemistry*, 266(13):8050–8054.

Lisman, J., Schulman, H., and Cline, H. (2002). The molecular basis of CaMKII function in synaptic and behavioural memory. *Nature Reviews Neuroscience*, 3(3):175–190.

Manninen, T., Hituri, K., Kotaleski, J. H., Blackwell, K. T., and Linne, M.-L. (2010). Postsynaptic signal transduction models for long-term potentiation and depression. *Frontiers in Computational Neuroscience*, 4.

Nishiyama, M., Hoshino, A., Tsai, L., Henley, J. R., Goshima, Y., Tessier-Lavigne, M., Poo, M.-M., and Hong, K. (2003). Cyclic AMP/GMP-dependent modulation of Ca2+ channels sets the polarity of nerve growth-cone turning. *Nature*, 423(6943):990–995.

Song, H., Ming, G., He, Z., Lehmann, M., McKerracher, L., Tessier-Lavigne, M., and Poo, M. (1998). Conversion of neuronal growth cone responses from repulsion to attraction by cyclic nucleotides. *Science*, 281(5382):1515–1518.

Song, H. J. and Poo, M. M. (1999). Signal transduction underlying growth cone guidance by diffusible factors. *Current Opinion in Neurobiology*, 9(3):355–363.

Stemmer, P. M. and Klee, C. B. (1994). Dual calcium ion regulation of calcineurin by calmodulin and calcineurin B. *Biochemistry*, 33(22):6859–6866.

Zhabotinsky, A. M. (2000). Bistability in the Ca(2+)/calmodulin-dependent protein kinase-phosphatase system. *Biophysical journal*, 79(5):2211–21.